



Cite this: DOI: 10.1039/c7nj02260c

Improving photocatalytic reduction of 4-nitrophenol over ZrO₂–TiO₂ by synergistic interaction between methanol and sulfite ions†

Diana Guerrero-Araque,^a Próspero Acevedo-Peña,^b David Ramírez-Ortega^c and Ricardo Gómez^a

The effect of two sacrificial agents (methanol and sodium sulfite) on the photocatalytic reduction of 4-nitrophenol employing a ZrO₂–TiO₂ photocatalyst is reported. The experimental results showed a decrease in the generation of OH• radicals and diminution in the charge transfer resistance that favor the electron transfer toward 4-nitrophenolate ions. Based on the results, it is possible to establish that methanol acts as a hole scavenger while sulfite ions act as radical scavengers, improving the reduction from 4-nitrophenol to 4-aminophenol. The synergistic effect has been corroborated by photoluminescence and photoelectrochemical measurements.

Received 24th June 2017,
Accepted 11th September 2017

DOI: 10.1039/c7nj02260c

rsc.li/njc

Introduction

The synthesis of compounds of commercial interest using heterogeneous photocatalysis is an attractive alternative for the transformation of organic compounds by oxidation and/or reduction processes.^{1–5} In particular, it has been proposed to reduce 4-nitrophenol to 4-aminophenol because the latter is a precursor for the synthesis of different pharmaceutical products.^{6,7}

Among various photocatalysts, TiO₂ is the most widely used due to its low toxicity, high corrosion resistance and low cost. However, this semiconductor has thermodynamic and kinetic limitations, which affect the reduction process of 4-nitrophenol. Electrons photogenerated in the conduction band of TiO₂ do not have enough potential to efficiently reduce the molecule of 4-nitrophenol.⁸ Otherwise, the photogenerated holes in TiO₂ are highly oxidizing, causing the fast oxidation of organic molecules including 4-nitrophenol.^{9–11}

Therefore, to improve the photocatalytic activity of TiO₂ in reduction processes various strategies have been employed, for example, supporting metal nanoparticles such as Ag, Au, Pt or Ir, which act as co-catalysts. In these cases, the rate of reaction increases significantly in comparison to TiO₂ alone;⁷ nevertheless, this strategy is not profitable due to the high cost

of noble metals.^{12–16} Another strategy comprises coupling of TiO₂ with other semiconductors to create heterojunctions that improve the electron–hole pair separation and separate reduction and oxidation sites. Also, semiconductors with a more negative conduction band allow obtaining electrons of a greater reductive potential. For example, materials such as TiO₂–CdS,¹⁷ TiO₂–Cu₂O,¹⁸ BiOBr–TiO₂,¹⁹ and ZrO₂–TiO₂^{20–22} have been employed successfully in reduction reactions. Specifically, the addition of ZrO₂ has attracted much attention in recent years due to its wide band gap and highly reductive electrons in its conduction band.^{23,24} In a previous study, the material with 5 mol% of ZrO₂ presented the best behavior attributed to surface states at the interface of ZrO₂–TiO₂ heterojunctions. These surface states act as traps for charge carriers favoring the spatial separation of electron–hole pairs.²⁵

In addition, to avoid the competition of photogenerated oxidizing holes in the reduction of 4-nitrophenol, sacrificial agents, such as Na₂SO₃ and hydrazine, have been used as hole scavengers.^{26–28} These compounds can be adsorbed on TiO₂, so their role during the photocatalytic reduction of 4-nitrophenol can go beyond acting as hole scavengers.²⁹ Despite the addition of these compounds to the reaction medium, the photocatalytic reduction of 4-nitrophenol on TiO₂ is very slow, requiring more than 3 hours to reduce 15 ppm of the compound, namely 6 times slower than photocatalysts like CdS.^{30,31}

On the other hand, a strategy widely used for H₂ production from water splitting over TiO₂ is the addition of alcohols as sacrificial agents.^{32,33} These alcohols act as hole traps decreasing the recombination process of TiO₂ and leaving more electrons available to be transferred to the solution. Mahdavi *et al.*³⁴ studied the photocatalytic reduction of aromatic nitro compounds in

^a Universidad Autónoma Metropolitana, Departamento de Química, Av. San Rafael Atlixco 156, P.C. 09340, Mexico City, Mexico. E-mail: dianacga@msn.com

^b CONACyT-Centro de Investigación en Ciencia Aplicada y Tecnología Avanzada-Unidad Legaria, IPN, 11500, Mexico City, Mexico

^c Centro de Ciencias Aplicadas y Desarrollo Tecnológico, Universidad Nacional Autónoma de México, Circuito Exterior S/N, Ciudad Universitaria, P.O. Box 70-186, Coyoacán 04510, D.F., Mexico

† Electronic supplementary information (ESI) available. See DOI: 10.1039/c7nj02260c

the presence of ethanol, and established that alcohol oxidation and reduction of the nitro compound occur at the same time. Challagulla *et al.* compared the rates of reduction of 4-nitrophenol in the presence of primary and secondary alcohols evidencing the highest rate by primary alcohols.³⁵ Nevertheless, there does not exist any study on the reduction of 4-nitrophenol using a photocatalyst with the addition of two sacrificial agents recognized as hole scavengers.

Therefore, we report the photocatalytic reduction of 4-nitrophenol over the ZrO₂-TiO₂ photocatalyst in the presence of two sacrificial agents (sodium sulfite and methanol). To clarify the impact of each sacrificial agent involved in the photocatalytic reduction, fluorescence spectroscopy and (photo)electrochemical measurements were performed.

Experimental

Synthesis of the ZrO₂-TiO₂ photocatalyst

The ZrO₂-TiO₂ photocatalyst was synthesized by means of the sol-gel method as reported elsewhere.²⁵ In brief, the precursor solution was a mixture of titanium *n*-butoxide, zirconium *n*-butoxide (5 mol% of ZrO₂), *n*-butanol and nitric acid. The mixture was refluxed at 353 K for 16 hours under constant stirring. Then, the solid was dried and calcined at 773 K for 4 hours.

Characterization

The ZrO₂-TiO₂ photocatalyst was characterized using a Bruker D2 Phaser diffractometer with CuK α radiation = 0.15418 nm. The absorption spectrum was recorded using a Varian Cary 100 Spectrophotometer equipped with an integrating sphere. The textural analysis was carried out on a Quantachrome Autosorb 3B. The SEM-EDS images of the sample were obtained on a Jeol7600F microscope.

Photocatalytic reduction

The photocatalytic reactions were carried out using a home-made reactor with 200 ml of four electrolytes: water (H₂O), methanol/water (MeOH/H₂O), water/sulfite ions (H₂O/SO₃²⁻), methanol/water/sulfite ions (MeOH/H₂O/SO₃²⁻), all containing 10 ppm of 4-nitrophenol and 150 mg of the photocatalyst. 100 mg of the electrolytes with sodium sulfite (Na₂SO₃²⁻) were used and in the case of the presence of methanol, the methanol/water mixtures were 25:75 vol% (the amounts used were previously optimized). Prior to irradiation, the mixtures were stirred in the dark for 30 min to facilitate the adsorption-desorption equilibrium. The mixtures were illuminated using a mercury lamp enclosed in a quartz tube submerged at the center of the reactor ($\lambda = 254$ nm, $I_0 = 7.6$ mW cm⁻²). The photocatalytic reduction was monitored using a Varian Cary 100 spectrophotometer followed by the disappearance of the absorption band at 400 nm corresponding to the 4-nitrophenolate ion.

Electrochemical characterization

The ZrO₂-TiO₂ photocatalyst was supported on Ti plates following the procedure reported previously.^{36,37} Electrochemical

measurements were carried out on a conventional three-electrode cell equipped with a quartz window (1.23 cm²) that allows UV light irradiation. The Ag/AgCl/3M KCl electrode was used as a reference electrode. The counter electrode was a graphite rod and the ZrO₂-TiO₂ film as the working electrode. The experiments were carried out in four electrolytes: H₂O, MeOH/H₂O, H₂O/SO₃²⁻, MeOH/H₂O/SO₃²⁻, all containing 0.03 M KClO₄ as the supporting electrolyte and adjusting the pH to 9.2. Before each measurement N₂ was bubbled. The semiconductor properties were estimated from Mott-Schottky plots, the space charge capacitance of the films was measured in the dark ($\nu = 20$ mV s⁻¹) and at a frequency of 400 Hz. For the (photo)electrochemical measurements an Autolab PGSTAT 302N potentiostat was used.

Results and discussion

The roles of methanol and sodium sulfite were studied in the photocatalytic reduction of 4-nitrophenol over the ZrO₂-TiO₂ photocatalyst (5 mol% ZrO₂) obtained by the sol-gel method. The XRD pattern of the ZrO₂-TiO₂ photocatalyst (ZT) only shows the anatase phase of TiO₂ (see Fig. S1, ESI[†]). Nevertheless, in this sample the two components form ZrO₂-TiO₂ heterojunctions as has been reported in a previous study.²⁵ For comparison, pristine TiO₂ and ZrO₂ obtained by the sol-gel method were included (Fig. S1 in ESI[†]).³⁸ The crystallite size (8.8 nm), band gap energy (3.2 eV) and specific surface area (147 m² g⁻¹) of the ZT photocatalyst were estimated using the Scherrer equation, a modified Kubelka-Munk function and the BET N₂ adsorption method, respectively (see Fig. S1-S3 and Table S1 in the ESI[†]). As can be seen from Fig. 1, the particles present a smooth surface and an irregular shape. The elemental composition of the material, obtained by SEM-EDS, shows a homogeneous distribution of Ti, O and Zr elements (Fig. 1).³⁹

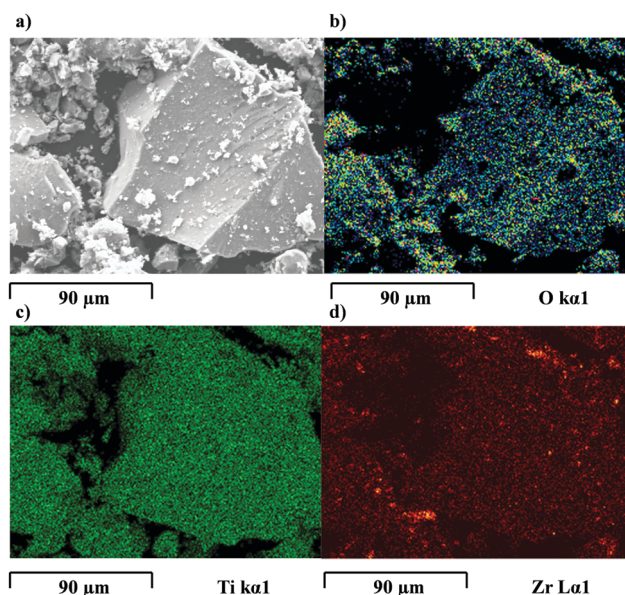


Fig. 1 (a-d) SEM image and EDX elemental mapping of O, Ti and Zr.

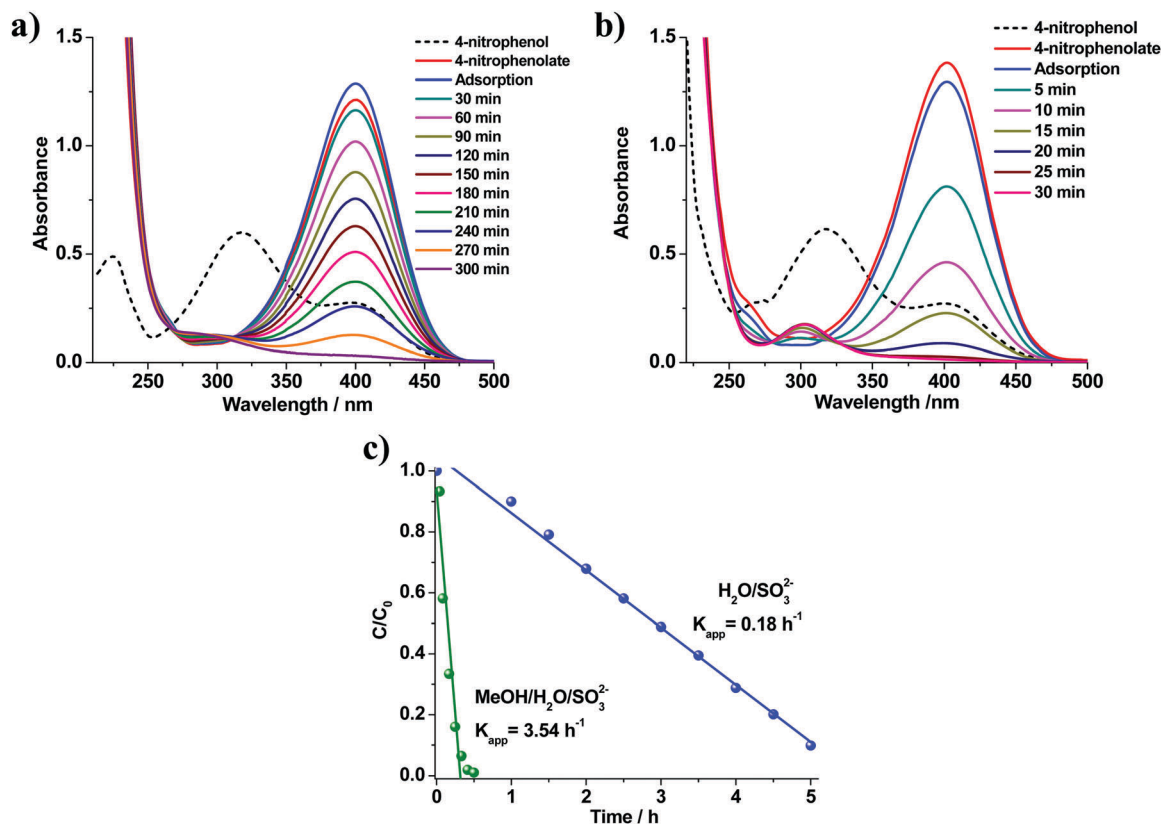


Fig. 2 UV-Vis spectra of 4-nitrophenol photoreduction with the $\text{ZrO}_2\text{-TiO}_2$ photocatalyst: (a) $\text{H}_2\text{O}/\text{SO}_3^{2-}$, (b) $\text{MeOH}/\text{H}_2\text{O}/\text{SO}_3^{2-}$; (c) zero order kinetic reaction fitting data for the photoreduction of 4-nitrophenol.

In order to study the effect of methanol (hole scavenger) on the photocatalytic reduction of 4-nitrophenol, 150 mg of the photocatalyst were suspended in 200 ml of the two electrolytes: water (H_2O) and methanol/water ($\text{MeOH}/\text{H}_2\text{O}$), both solutions containing 10 ppm of 4-nitrophenol. The suspensions were stirred in the dark for 30 min to ensure adsorption/desorption equilibrium. The evolution of solutions shows that the reduction of 4-nitrophenol does not occur, indicating that the presence of sodium sulfite is necessary for the reduction process, as previously reported.⁴⁰ To accomplish the photocatalytic reduction, 150 mg of the photocatalyst were suspended in 200 ml of the two electrolytes: water/sulfite ions ($\text{H}_2\text{O}/\text{SO}_3^{2-}$) and methanol/water/sulfite ions ($\text{MeOH}/\text{H}_2\text{O}/\text{SO}_3^{2-}$), both mixtures containing 10 ppm of 4-nitrophenol and 100 mg of sodium sulfite (Na_2SO_3). The mixtures were irradiated, and the results are reported in Fig. 2. Prior to the addition of sodium sulfite, the initial solution of 4-nitrophenol exhibited two bands at 315 and 400 nm corresponding to the balance between 4-nitrophenol and the 4-nitrophenolate ion, respectively. Subsequently, the solutions show two absorption bands: one at 210 nm, corresponding to the sulfite ions (SO_3^{2-}) and the other at 400 nm, characteristic of the 4-nitrophenolate ion due to the alkaline medium generated by the presence of Na_2SO_3 .⁴¹ To evaluate the photocatalytic reduction of 4-nitrophenol, disappearance of the absorption band at 400 nm (4-nitrophenolate ion) was monitored, and as a consequence, the formation of an absorption band at 300 nm

accompanied by two isosbestic points at 267 and 345 nm indicated the conversion of the 4-nitrophenolate ion to 4-aminophenol.^{42–46} The reduction of 4-nitrophenol in $\text{H}_2\text{O}/\text{SO}_3^{2-}$ shows a weak absorption band at 300 nm, which is commonly associated with 4-aminophenol. It is worth mentioning that the total reduction of 4-nitrophenol in this electrolyte is achieved after 5 h under illumination. This behavior is typically observed when TiO_2 is used in the absence of co-catalysts.⁴⁷ However, in the reaction carried out in the $\text{MeOH}/\text{H}_2\text{O}/\text{SO}_3^{2-}$ electrolyte the formation of the 4-aminophenol absorption band at 300 nm is clearly observed, confirming the presence of this compound.^{7,48–50} It is important to point out that the time of photoreduction to convert 1.043×10^{-5} moles of 4-nitrophenol decreases from more than 300 min (in the absence of methanol) to 30 min (in the presence of methanol). Also, at higher methanol concentrations there is no variation in the reduction kinetics of the 4-nitrophenolate ion. The reaction rate constant adjusted by a zero order kinetics increased 19 times in the $\text{MeOH}/\text{H}_2\text{O}/\text{SO}_3^{2-}$ electrolyte compared with the photoreduction performed in the $\text{H}_2\text{O}/\text{SO}_3^{2-}$ electrolyte (Fig. 2c). This drastic increase in the rate constant shows the important role of MeOH in this reaction, as it diminishes the competition between reduction and oxidation reactions with an effective decrease in the available holes (consumed by methanol), thus favoring the reduction process. In the same way, this can be associated with a larger amount of photogenerated electrons available for the reduction of

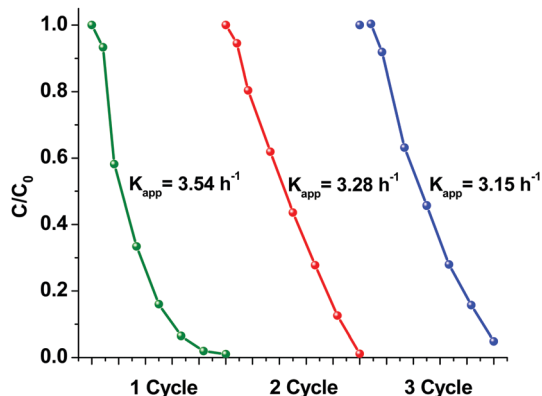


Fig. 3 Cycles of ZT photocatalyst in the photoreduction of 4-nitrophenol in the MeOH/H₂O/SO₃²⁻ electrolyte; the photocatalyst was regenerated at 773 K for 2 h.

4-nitrophenol. The reaction rate constant estimated for TiO₂ obtained by means of the sol-gel method is shown in Fig. S4 (ESI[†]). For TiO₂, the presence of methanol in the electrolyte also increased 25 times the reaction rate compared with the photoreduction performed in the H₂O/SO₃²⁻ electrolyte. However, the ZT photocatalyst shows the highest rate of reaction. Additionally, pristine ZrO₂ was evaluated in the photoreduction of 4-nitrophenol in the MeOH/H₂O/SO₃²⁻ electrolyte, but the reduction reaction did not proceed (Fig. S5 in the ESI[†]). In spite of this result, the presence of ZrO₂ in the ZT photocatalyst improves the textural properties of the material (see Table S1, ESI[†]), and decreases the rate of electron-hole pair recombination due to the formation of energetic states in the ZrO₂-TiO₂ heterojunctions.²⁵

To determine the stability of the ZT photocatalyst in the MeOH/H₂O/SO₃²⁻ electrolyte, the material was evaluated during 3 cycles (Fig. 3). The estimated reaction rate constant shows a slight decrease, proving that the ZT material has good photostability in the reaction.

These results could seem ambiguous, which is reflected in the fact that the addition of two compounds widely recognized as hole scavengers (MeOH and SO₃²⁻ ions) generates such a remarkable increase in the reaction rate. In order to clarify the role of SO₃²⁻ ions and MeOH during the reduction of 4-nitrophenol, (photo)electrochemical characterization was performed. Initially, the impact of methanol and/or SO₃²⁻ ions on the semiconducting properties of the material was studied. For this purpose, ZrO₂-TiO₂ photocatalyst films were exposed to 4 electrolytes: H₂O, MeOH/H₂O, H₂O/SO₃²⁻, and MeOH/H₂O/SO₃²⁻. Fig. 4 shows the Mott-Schottky curves, where the material exhibits an *n*-type behavior. The less negative potential value corresponds to the film exposed to H₂O ($E_{fb} = -0.67$ V). The methanol addition generates a slight shift towards a more negative value than H₂O ($E_{fb} = -0.69$ V), which was associated with methanol adsorption over the photocatalyst and subsequent formation of superficial methoxy groups.^{51,52} At the same time, the presence of SO₃²⁻ ions in H₂O/SO₃²⁻ and MeOH/H₂O/SO₃²⁻ electrolytes provokes a shift towards more negative potential values, with E_{fb} values of -0.79 and -0.89 V, respectively.

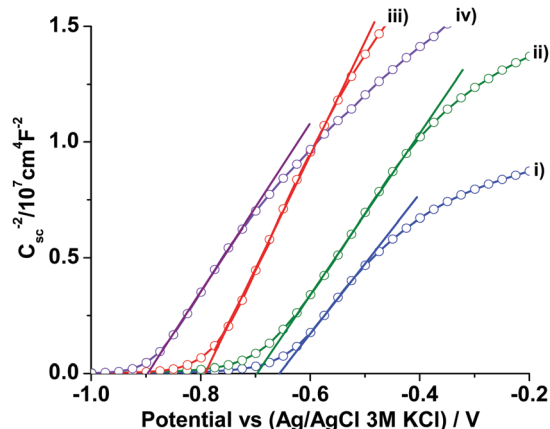


Fig. 4 Mott-Schottky plots of the ZrO₂-TiO₂ photocatalyst in (i) H₂O, (ii) MeOH/H₂O, (iii) H₂O/SO₃²⁻ and (iv) MeOH/H₂O/SO₃²⁻. The C_{sc} values were obtained at 400 Hz.

This behavior shows that SO₃²⁻ ions present strong specific adsorption on the material. The presence of MeOH causes this adsorption to be even greater, modifying notably the flat band potential of the semiconductor.^{53,54}

Measurements of the photocurrent generated by the film allow discerning whether these two agents act as hole scavengers which would be reflected as an increase in the photocurrent compared to a solution without hole scavengers.⁵⁵⁻⁵⁷ The current generation under illumination was evaluated by imposing a potential of 0.3 V to promote electron transport towards the substrate, using the following electrolytes: H₂O, MeOH/H₂O, H₂O/SO₃²⁻, and MeOH/H₂O/SO₃²⁻ (Fig. 5). In this sense, H₂O and H₂O/SO₃²⁻ measurements exhibit similar low stable photocurrents, indicating that SO₃²⁻ ions do not act as hole scavengers.

In contrast, the results in the MeOH/H₂O electrolyte are considerably higher, confirming that this alcohol acts as a hole scavenger.⁵⁸ Likewise, the response is fastest when MeOH and SO₃²⁻ ions are present, resulting in the highest photocurrent, associated with the synergistic action between methanol and

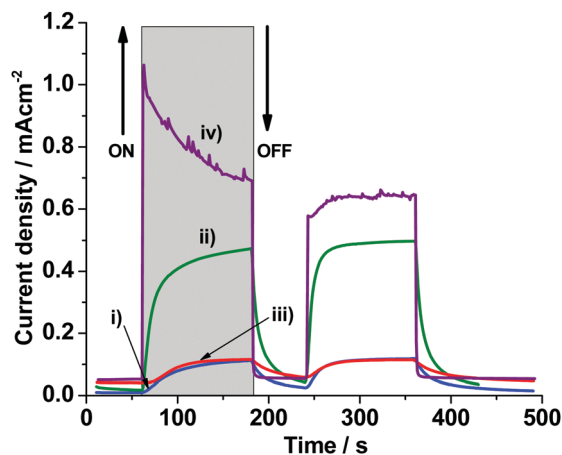


Fig. 5 Photocurrent response under the UV light on-off process at an applied voltage of 0.3 V (vs. Ag/AgCl) measured by employing ZrO₂/TiO₂ films in: (i) H₂O, (ii) MeOH/H₂O, (iii) H₂O/SO₃²⁻ and (iv) MeOH/H₂O/SO₃²⁻.

sulfite ions. It is noteworthy that although the photocurrent decreases in the MeOH/H₂O/SO₃²⁻ electrolyte in the second pulse, it is higher than that in the other electrolytes. These results show that methanol acts as a hole scavenger on the photocatalyst surface, reducing the recombination of electron hole pairs and thus benefiting the photocatalytic activity of the material.⁵⁹

In order to complement the chronoamperometric results obtained previously, the photocatalytic generation of OH• radicals was measured by terephthalic acid fluorescence tests (Fig. 6).^{60,61} In the reaction with OH• radicals, terephthalic acid becomes 2-hydroxyterephthalic acid, which emits a single fluorescence signal at 426 nm. When the photocatalyst is exposed to the H₂O electrolyte, the fluorescence signal corresponding to the generation of OH• radicals increases with illumination time, Fig. 6a. On the other hand, the fluorescence signal in the MeOH/H₂O electrolyte, though lower in intensity than that observed in H₂O, increases over time showing that MeOH decreases the generation of OH• radicals upon illumination of the photocatalyst. This is associated with the fact that methanol reacts with the holes photogenerated on the photocatalyst surface (Fig. 6b).⁶²⁻⁶⁴ In addition, when SO₃²⁻ ions are present in H₂O and MeOH/H₂O electrolytes, the number of OH• radicals is fewer, which shows that although this agent does not react with the holes at the photocatalyst surface, Fig. 5, it has a scavenging effect on OH• radicals in solution. Noteworthily, the intensity band is much lower in the MeOH/H₂O/SO₃²⁻ electrolyte, due to the synergistic effect of these two agents (MeOH and SO₃²⁻), which controls the amount of OH• radicals

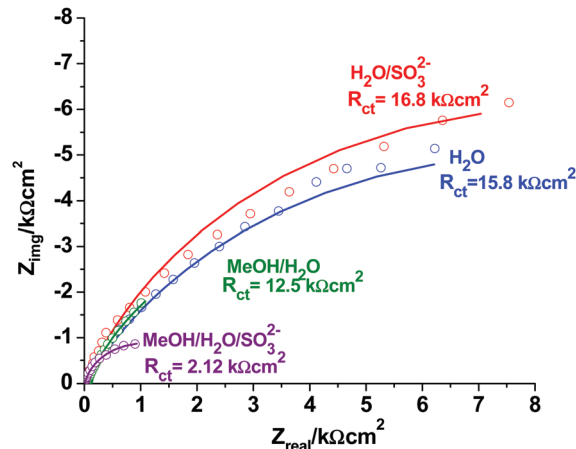


Fig. 7 Electrochemical impedance spectra for H₂O, MeOH/H₂O, H₂O/SO₃²⁻ and MeOH/H₂O/SO₃²⁻.

in the reaction medium. Based on the obtained results, it can be assumed that the slight reduction in the absorption band at 210 nm reported during the photocatalytic tests, associated with SO₃²⁻ ions, can be related to OH• radicals consumed upon photocatalyst illumination.⁶⁵ Additionally, fluorescence results in H₂O and MeOH/H₂O electrolytes in the absence of the photocatalyst are included in Fig. S6 in the ESI.†

Finally, to demonstrate the impact of electrolyte composition on the interfacial charge transfer process and confirm the role of MeOH and SO₃²⁻ in the photocatalytic reaction, electrochemical

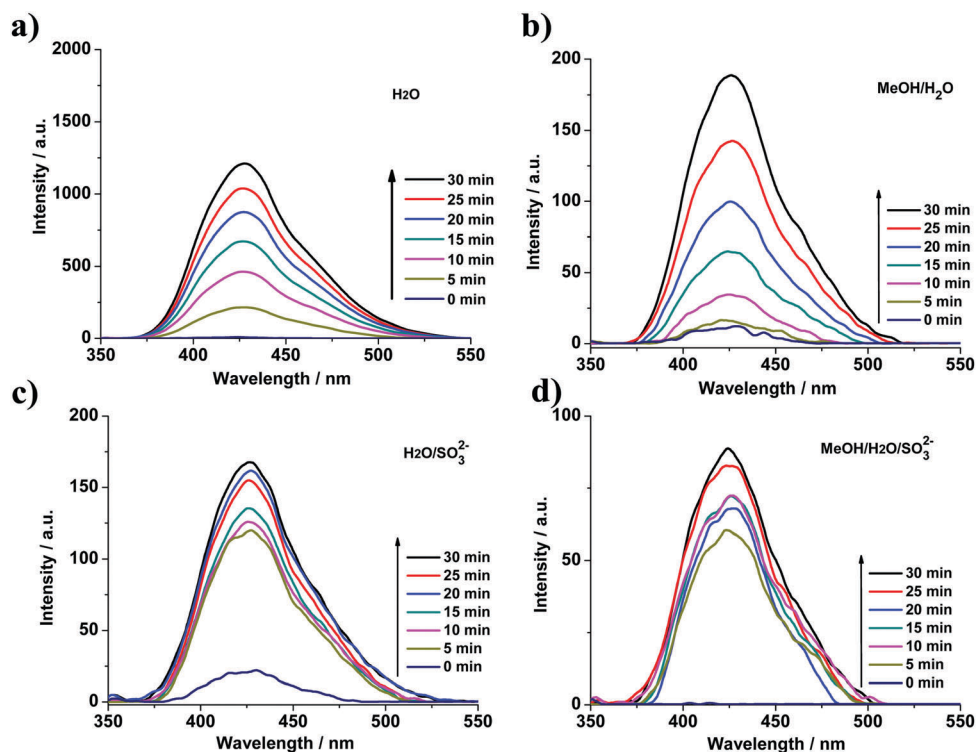


Fig. 6 Fluorescence spectra of terephthalic acid solutions with the ZrO₂/TiO₂ photocatalyst under UV light in four electrolytes: (a) H₂O, (b) MeOH/H₂O, (c) H₂O/SO₃²⁻ and (d) MeOH/H₂O/SO₃²⁻.

impedance spectroscopy was used under illumination.²⁵ In this way, the overall process includes transfer resistance in the material (oxidation and reduction) under similar conditions in which the photocatalyst is employed (Fig. 7).

The H₂O and H₂O/SO₃²⁻ electrolytes have the highest resistance. In the latter, the presence of SO₃²⁻ ions generates a slightly higher resistance. It is important to mention that the H₂O electrolyte promotes the oxidation of the 4-nitrophenolate ion, while the H₂O/SO₃²⁻ electrolyte favors the reduction process, which indicates that SO₃²⁻ ions seem to act as electron transfer mediators towards 4-nitrophenol. The charge transfer resistance observed in the H₂O/SO₃²⁻ electrolyte is related to chronoamperometry results, which show that sulfite ions are

effective sacrificial agents that react with OH• radicals in solution and do not act as photogenerated hole scavengers. Moreover, the low resistance in the MeOH/H₂O electrolyte confirms that the charge transfer is favored at the photocatalyst/solution interface. However, although there is a decrease in the charge transfer resistance in this electrolyte, this mixture favors 4-nitrophenol oxidation. Additionally, in the MeOH/H₂O/SO₃²⁻ electrolyte, a smaller charge transfer resistance is obtained due to the synergistic action of MeOH and SO₃²⁻ ions, where the hole scavenger (MeOH) increases the amount of photogenerated electrons at the photocatalyst surface, and SO₃²⁻ ions react with OH• radicals and promote electron transfer toward 4-nitrophenol.

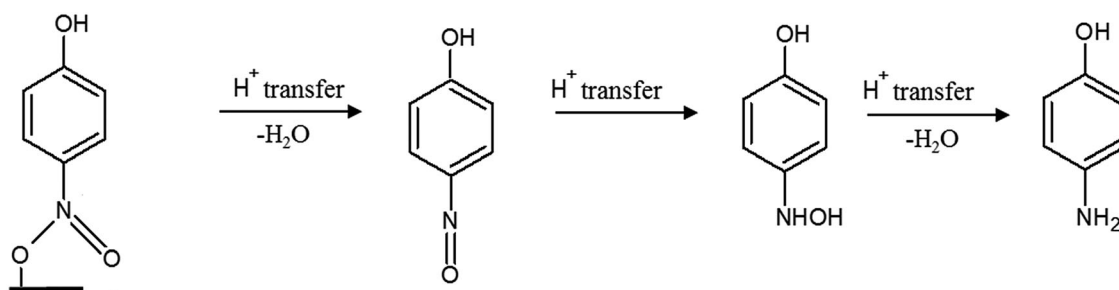


Fig. 8 Proposed mechanism for the photocatalytic reduction of 4-nitrophenol to 4-aminophenol.

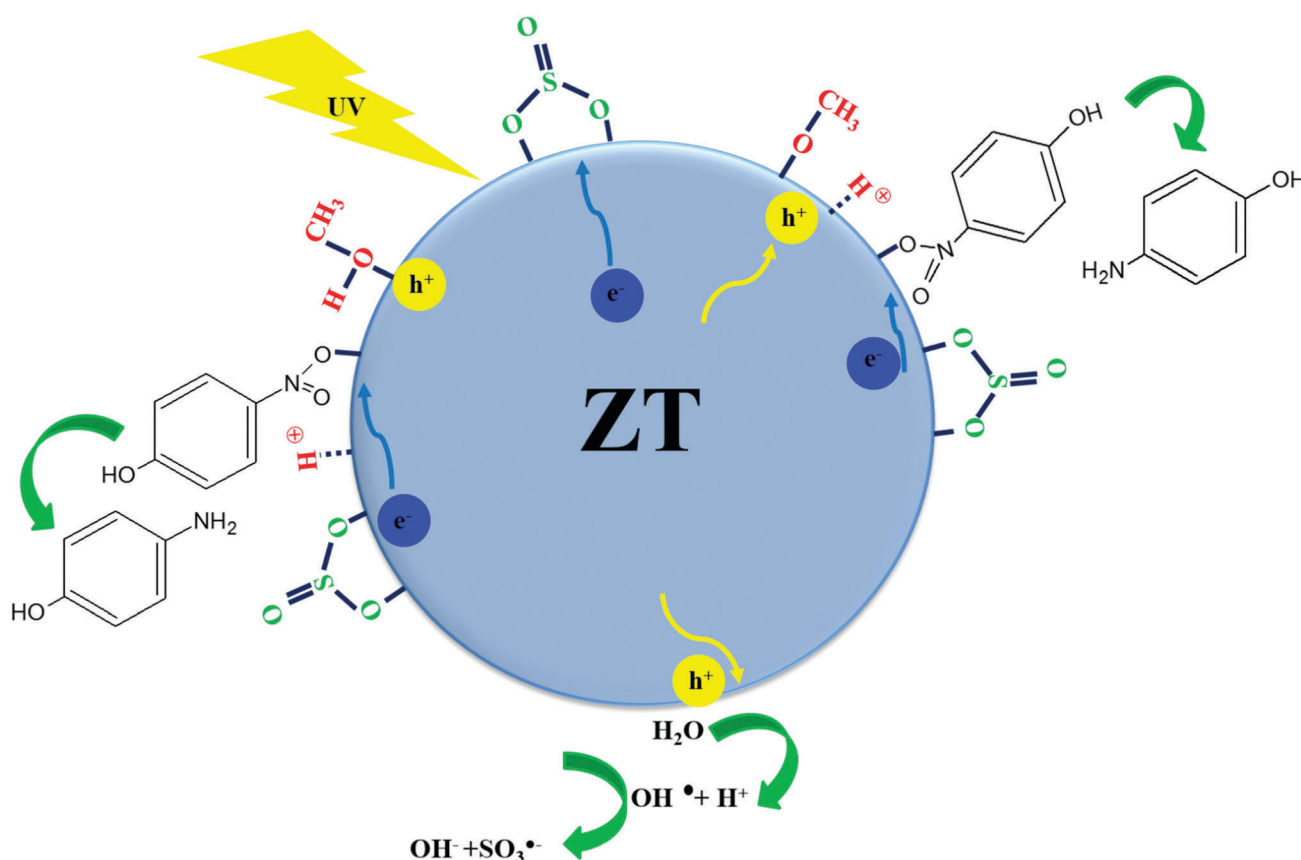
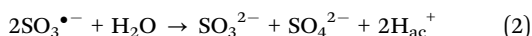
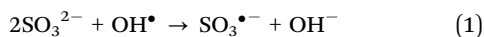


Fig. 9 Graphic representation of the 4-nitrophenol reduction using two sacrificial agents (methanol and sodium sulfite).

It is well known that it is difficult to investigate the reduction process in photocatalysis separately, because it is affected by the oxidation process, and their mutual competition affects the overall reaction rate. In this case, the 4-nitrophenolate ion, the sulfite ion and methanol are adsorbed on the ZT photocatalyst. At this stage, the coordinated interaction between 4-nitrophenolate ions, sulfite ions and methanol allows the formation of intermediates, which leads to the formation of 4-aminophenol (Fig. 8).⁶⁶ In this case, the addition of MeOH (in the presence of Na₂SO₃) favors the reduction of 4-nitrophenol causing a synergistic effect that leads to an increase in the reaction rate. During irradiation, the photogenerated holes can be captured by MeOH due to the specific adsorption of methanol on the material. The holes can be transferred from the photocatalyst to the methoxy groups (CH₃O), decreasing the amount of holes at the surface of the material.^{12,60,67–69} On the other hand, OH• radicals formed in the reaction medium are rapidly captured by SO₃²⁻ ions adsorbed on the surface of the photocatalyst or in the solution, generating a partial oxidation to SO₄²⁻ (reactions (1) and (2)).⁷⁰



In addition, the specific adsorption of SO₃²⁻ ions onto TiO₂ and ZT materials propitiates the transfer of photogenerated electrons toward the 4-nitrophenolate ion (Fig. 9). Thus, these two agents act together to avoid the oxidation of the formed 4-nitrophenolate ion or 4-aminophenol, giving rise to an increase in the band associated with 4-aminophenol. This phenomenon can be related to the fact that the adsorption of SO₃²⁻ ions over the photocatalyst generates electrons with a more reducing potential and provokes a major separation between the flat band potential of the material and the redox potential of the 4-nitrophenol/4-aminophenol couple (−0.76 V: considering this value in aqueous solution).²⁷

Thus, the MeOH/H₂O/SO₃²⁻ electrolyte enhanced the reduction process of the 4-nitrophenolate ion by increasing the reaction rate 19 times compared to the H₂O/SO₃²⁻ electrolyte (Fig. 2). In fact, the addition of methanol achieved higher rate constants than any other TiO₂ in the absence of co-catalysts, as has been previously reported. The results of this study are comparable with the results obtained under similar conditions, but show improved reaction rates with respect to TiO₂ and TiO₂ with metal cocatalysts.^{26,27,29,71,72}

Conclusions

The addition of a hole scavenger, such as methanol, proved to be an effective strategy to accelerate the reduction process of 4-nitrophenol in the presence of sodium sulfite, increasing the reaction rate 19 times for the ZrO₂-TiO₂ photocatalyst. Electrochemical characterization shows that the presence of sulfite ions and methanol in the solution provokes a displacement of the flat band potential towards more negative values generating electrons with a higher reducing potential. This behavior, associated with the strong adsorption of these species

on the surface of the material is greater when the two agents are present in the solution. On the other hand, monitoring of the generation of oxidizing species (OH• radicals) shows that methanol and sulfite ions decrease the amount of these oxidant species upon photocatalyst illumination. Finally, characterization by EIS confirmed that the sulfite ion does not modify considerably charge transfer resistance in the photocatalytic process, as methanol does. However, charge-transfer resistance notoriously diminishes when both agents are present in the solution.

Conflicts of interest

There are no conflicts to declare.

Acknowledgements

Diana Guerrero-Araque gratefully acknowledges the support of a CONACYT scholarship CVU No. 506795. David Ramirez-Ortega with the CVU. No. 329398 thanks CONACYT for the grant given to pursue postdoctoral research.

References

- 1 C. Xu, Y. Yuan, R. Yuan and X. Fu, *RSC Adv.*, 2013, **3**, 18002–18008.
- 2 Z. Lu, Z. Zhu, D. Wang, Z. Ma, W. Shi, Y. Yan, X. Zhao, H. Dong, L. Yang and Z. Hua, *Catal. Sci. Technol.*, 2016, **6**, 1367–1377.
- 3 Z. Lu, X. Zhao, Z. Zhu, Y. Yan, W. Shi, H. Dong, Z. Ma, N. Gao, Y. Wang and H. Huang, *Chem. – Eur. J.*, 2015, **21**, 18528–18533.
- 4 Z. Lu, F. Chen, M. He, M. Song, Z. Ma, W. Shi, Y. Yan, J. Lan, F. Li and P. Xiao, *Chem. Eng. J.*, 2014, **249**, 15–26.
- 5 Z. Lu, P. Huo, Y. Luo, X. Liu, D. Wu, X. Gao, C. Li and Y. Yan, *J. Mol. Catal. A: Chem.*, 2013, **378**, 91–98.
- 6 H.-Q. Wang, J.-P. Yan, Z.-M. Zhang and W.-F. Chang, *React. Kinet. Catal. Lett.*, 2009, **97**, 91–99.
- 7 S. Gazi and R. Ananthakrishnan, *Appl. Catal., B*, 2011, **105**, 317–325.
- 8 S. Chen and L.-W. Wang, *Chem. Mater.*, 2012, **24**, 3659–3666.
- 9 Y. Tamaki, A. Furube, M. Murai, K. Hara, R. Katoh and M. Tachiya, *J. Am. Chem. Soc.*, 2006, **128**, 416–417.
- 10 D. Wiedmer, E. Sagstuen, K. Welch, H. J. Haugen and H. Tiainen, *Appl. Catal., B*, 2016, **198**, 9–15.
- 11 S.-Y. Lee and S.-J. Park, *J. Ind. Eng. Chem.*, 2013, **19**, 1761–1769.
- 12 T. Aditya, A. Pal and T. Pal, *Chem. Commun.*, 2015, **51**, 9410–9431.
- 13 J. Liang, A. Yue, Q. Wang, S. Song and L. Li, *RSC Adv.*, 2016, **6**, 29497–29503.
- 14 M. M. Mohamed and M. S. Al-Sharif, *Appl. Catal., B*, 2013, **142–143**, 432–441.
- 15 S. M. El-Sheikh, A. A. Ismail and J. F. Al-Sharab, *New J. Chem.*, 2013, **37**, 2399–2407.

- 16 M. Lei, W. Wu, S. Yang, X. Zhang, Z. Xing, F. Ren, X. Xiao and C. Jiang, *Part. Part. Syst. Charact.*, 2016, **33**, 212–220.
- 17 A. A. Beigi, S. Fatemi and Z. Salehi, *J. CO₂ Util.*, 2014, **7**, 23–29.
- 18 M. E. Aguirre, R. Zhou, A. J. Eugene, M. I. Guzman and M. A. Grela, *Appl. Catal., B*, 2017, **217**, 485–493.
- 19 Y. Zhao, X. Huang, X. Tan, T. Yu, X. Li, L. Yang and S. Wang, *Appl. Surf. Sci.*, 2016, **365**, 209–217.
- 20 M. C. Hidalgo, G. Colón, J. A. Navio, M. Macias, V. V. Kriventsov, D. I. Kochubey and M. V. Tsodikov, *Catal. Today*, 2007, **128**, 245–250.
- 21 C.-C. Lo, C.-H. Hung, C.-S. Yuan and J.-F. Wu, *Sol. Energy Mater. Sol. Cells*, 2007, **91**, 1765–1774.
- 22 L. Matějová, K. Kočí, M. Reli, L. Čapek, V. Matějka, O. Šolcová and L. Obalová, *Appl. Surf. Sci.*, 2013, **285P**, 688–696.
- 23 L. Renuka, K. S. Anantharaju, Y. S. Vidya, H. P. Nagaswarupa, S. C. Prashantha, S. C. Sharma, H. Nagabhushana and G. P. Darshan Grela, *Appl. Catal., B*, 2017, **210**, 97–115.
- 24 Y. Xu and M. A. A. Schoonen, *Am. Mineral.*, 2000, **85**, 543–556.
- 25 D. Guerrero-Araque, D. Ramírez-Ortega, P. Acevedo-Peña, F. Tzompantzi, H. A. Calderón and R. Gómez, *J. Photochem. Photobiol., A*, 2017, **335**, 276–286.
- 26 A. Hernández-Gordillo, M. Arroyo, R. Zanella and V. Rodríguez-González, *J. Hazard. Mater.*, 2014, **268**, 84–91.
- 27 A. Hernández-Gordillo, S. Obregón, F. Paraguay-Delgado and V. Rodríguez-González, *RSC Adv.*, 2015, **5**, 15194–15197.
- 28 T. K. Ghorai, *J. Mater. Res. Technol.*, 2015, **4**, 133–143.
- 29 S. Cipagauta, A. Hernández-Gordillo and R. Gómez, *J. Sol-Gel Sci. Technol.*, 2014, **72**, 428–434.
- 30 A. Hernández-Gordillo, A. G. Romero, F. Tzompantzi and R. Gómez, *Powder Technol.*, 2013, **250**, 97–102.
- 31 M. Ni, M. K. H. Leung, D. Y. C. Leung and K. Sumathy, *Renewable Sustainable Energy Rev.*, 2007, **11**, 401–425.
- 32 W.-C. Lin, W.-D. Yang, I.-L. Huang, T.-S. Wu and Z.-J. Chung, *Energy Fuels*, 2009, **23**, 2192–2196.
- 33 Z. Wang, Q. Hao, X. Mao, C. Zhou, D. Dai and X. Yang, *Phys. Chem. Chem. Phys.*, 2016, **18**, 10224–10231.
- 34 F. Mahdavi, T. C. Bruton and Y. Li, *J. Org. Chem.*, 1993, **58**, 744–746.
- 35 S. Challagulla, R. Nagarjuna, R. Ganesan and S. Roy, *J. Porous Mater.*, 2015, **22**, 1105–1110.
- 36 D. Ramírez-Ortega, A. M. Meléndez, P. Acevedo-Peña, I. González and R. Arroyo, *Electrochim. Acta*, 2014, **140**, 541–549.
- 37 D. Ramírez-Ortega, P. Acevedo-Peña, F. Tzompantzi, R. Arroyo, F. González and I. González, *J. Mater. Sci.*, 2017, **52**, 260–275.
- 38 H. Xu, S. Ouyang, P. Li, T. Kako and J. Ye, *ACS Appl. Mater. Interfaces*, 2013, **5**, 1348–1354.
- 39 J. Zhan, L. Li, Z. Xiao, D. Liu, S. Wang, J. Zhang, Y. Hao and W. Zhang, *ACS Sustainable Chem. Eng.*, 2016, **4**, 2037–2046.
- 40 A. Hernández-Gordillo, A. G. Romero, F. Tzompantzi and R. Gómez, *Appl. Catal., B*, 2014, **144**, 507–513.
- 41 S. Naraginti, F. B. Stephen, A. Radhakrishnan and A. Sivakumar, *Spectrochim. Acta, Part A*, 2015, **135**, 814–819.
- 42 K. Hareesh, R. P. Joshi, D. V. Sunitha, V. N. Bhoraskar and S. D. Dhole, *Appl. Surf. Sci.*, 2016, **389**, 1050–1055.
- 43 X. Du, J. He, J. Zhu, L. Sun and S. An, *Appl. Surf. Sci.*, 2012, **258**, 2717–2723.
- 44 B. Naik, S. Hazra, V. S. Prasad and N. N. Ghosh, *Catal. Commun.*, 2011, **12**, 1104–1108.
- 45 S. Jana, S. K. Ghosh, S. Nath, S. Pande, S. Praharaj, S. Panigrahi, S. Basu, T. Endo and T. Pal, *Appl. Catal., A*, 2006, **313**, 41–48.
- 46 Y. Zhu, J. Shen, K. Zhou, C. Chen, X. Yang and C. Li, *J. Phys. Chem. C*, 2011, **115**, 1614–1619.
- 47 C. Castañeda, F. Tzompantzi and R. Gómez, *J. Sol-Gel Sci. Technol.*, 2016, **80**, 426–435.
- 48 C. Kästner and A. F. Thünemann, *Langmuir*, 2016, **32**, 7383–7391.
- 49 K. Kuroda, T. Ishida and M. Harut, *J. Mol. Catal. A: Chem.*, 2009, **298**, 7–11.
- 50 C. Kastner and A. F. Thunemann, *Langmuir*, 2016, **32**, 7383–7391.
- 51 D. Wu, Y. Zhang, M. Wen, H. Fang and Q. Wu, *Inorg. Chem.*, 2017, **56**, 5152–5157.
- 52 A. Roy, B. Debnath, R. Sahoo, T. Aditya and T. Pal, *J. Colloid Interface Sci.*, 2017, **493**, 288–294.
- 53 C. Zhou, Z. Ren, S. Tan, Z. Ma, X. Mao, D. Dai, H. Fan, X. Yang, J. LaRue, R. Cooper, A. M. Wodtke, Z. Wang, Z. Li, B. Wang, J. Yang and J. Hou, *Chem. Sci.*, 2010, **1**, 575–580.
- 54 S. Liu, A.-A. Liu, B. Wen, R. Zhang, C. Zhou, L.-M. Liu and Z. Ren, *Chem. Phys. Lett.*, 2015, **6**, 3327–3334.
- 55 H. Kusama, H. Orita and H. Sugihara, *Langmuir*, 2008, **24**, 4411–4419.
- 56 L. Sang, H. Tan, X. Zhang, Y. Wu, C. Ma and C. Burda, *J. Phys. Chem. C*, 2012, **116**, 18633–18640.
- 57 H. K. Dunn, J. M. Feckl, A. Müller, D. Fattakhova-Rohlfing, S. G. Morehead, J. Roos, L. M. Peter, C. Scheu and T. Bein, *Phys. Chem. Chem. Phys.*, 2014, **16**, 24610–24620.
- 58 J. A. Byrne, B. R. Eggins, S. Linquette-Mailley and P. S. M. Dunlop, *Analyst*, 1998, **123**, 2007–2012.
- 59 L. Yu, H. Ruan, Y. Zheng and D. Li, *Nanotechnology*, 2013, **24**, 375601.
- 60 W. Chu, W. A. Saidi, Q. Zheng, Y. Xie, Z. Lan, O. V. Prezhdo, H. Petek and J. Zhao, *J. Am. Chem. Soc.*, 2016, **138**, 13740–13749.
- 61 G. Liu, C. Sun, H. G. Yang, S. C. Smith, L. Wang, G. Q. Lu and H.-M. Cheng, *Chem. Commun.*, 2010, **46**, 755–757.
- 62 K.-I. Ishibashi, A. Fujishima, T. Watanabe and K. Hashimoto, *Electrochem. Commun.*, 2000, **2**, 207–210.
- 63 J. Zhang and Y. Nosaka, *Appl. Catal., B*, 2015, **166-167**, 32–36.
- 64 S. Liu, Z. Zhao and Z. Wang, *Photochem. Photobiol. Sci.*, 2007, **6**, 695–700.
- 65 T. Tan, D. Beydoun and R. Amal, *J. Photochem. Photobiol., A*, 2003, **159**, 273–280.
- 66 V. N. H. Nguyen, R. Amal and D. Beydoun, *Chem. Eng. Sci.*, 2003, **58**, 4429–4439.

- 67 W.-Z. Gao, Y. Xu, Y. Chen and W.-F. Fu, *Chem. Commun.*, 2015, **51**, 13217–13220.
- 68 C. Hammond, M. M. Forde, M. H. A. Rahim, A. Thetford, Q. He, R. L. Jenkins, N. Dimitratos, J. A. Lopez-Sanchez, N. F. Dummer, D. M. Murphy, A. F. Carley, S. H. Taylor, D. J. Willock, E. E. Stangland, J. Kang, H. Hagen, C. J. Kiely and G. J. Hutchings, *Angew. Chem., Int. Ed.*, 2012, **51**, 5129–5133.
- 69 G. Kolesov, D. Vinichenko, G. A. Tritsarlis, C. M. Friend and E. Kaxiras, *J. Phys. Chem. Lett.*, 2015, **6**, 1624–1627.
- 70 B. C. Faust, M. R. Hoffmann and D. W. Bahnemann, *J. Phys. Chem.*, 1989, **93**, 6371–6381.
- 71 X. Wang, F. Tan, W. Wang, X. Qiao, X. Qiu and J. Chen, *Chemosphere*, 2017, **172**, 147–154.
- 72 V. Brezová, A. Blazková, I. Surina and B. Havlinová, *J. Photochem. Photobiol., A*, 1997, **107**, 233–237.